Molecular Pharmacology Fast Forward. Published on July 2, 2022 as DOI: 10.1124/molpharm.122.000497
This article has not been copyedited and formatted. The final version may differ from this version.

Title: Michaelis-Menten quantification of ligand signalling bias applied to the promiscuous Vasopressin V2 receptor

Authors: Franziska Marie Heydenreich[1,2,3*], Bianca Plouffe[2,4], Aurélien Rizk[1], Dalibor Milić[1,5], Joris Zhou[2], Billy Breton[2], Christian Le Gouill[2], Asuka Inoue[6], Michel Bouvier[2,*] and Dmitry B. Veprintsev[1,7,8,*]

Affiliations:

[1]Laboratory of Biomolecular Research, Paul Scherrer Institute, 5232 Villigen PSI, Switzerland and Department of Biology, ETH Zürich, 8093 Zürich, Switzerland

[2]Department of Biochemistry and Molecular Medicine, Institute for Research in Immunology and Cancer, Université de Montréal, Montréal, Québec, Canada

[3]MRC Laboratory of Molecular Biology, Cambridge CB2 0QH, UK

[4]The Wellcome-Wolfson Institute for Experimental Medicine, School of Medicine, Dentistry and Biomedical Sciences, Queen's University Belfast, 97 Lisburn Road, Belfast, BT9 7BL, United Kingdom

[5]Department of Structural and Computational Biology, Max Perutz Labs, University of Vienna, Campus-Vienna-Biocenter 5, 1030 Vienna, Austria

[6]Graduate School of Pharmaceutical Sciences, Tohoku University, Sendai, Miyagi 980-8578, Japan.

[7]Centre of Membrane Proteins and Receptors (COMPARE), University of Birmingham and University of Nottingham, Midlands, UK.

[8]Division of Physiology, Pharmacology & Neuroscience, School of Life Sciences, University of Nottingham, Nottingham, NG7 2UH, UK.

[*]Corresponding authors. franziskah@mrc-lmb.cam.ac.uk, michel.bouvier@umontreal.ca, dmitry.veprintsev@nottingham.ac.uk

Molecular Pharmacology Fast Forward. Published on July 2, 2022 as DOI: 10.1124/molpharm.122.000497
This article has not been copyedited and formatted. The final version may differ from this version.

Running title: Michaelis Menten quantification of GPCR-G protein signalling

Corresponding author address:
Franziska M. Heydenreich
MRC Laboratory of Molecular Biology
Francis Crick Avenue
Cambridge CB2 0QH
United Kingdom

Phone: + 44 1223 267969
franziskah@mrc-lmb.cam.ac.uk

Additional corresponding authors:
Michel Bouvier
Dmitry B. Veprintsev

Text pages: 17
Number of Tables: 4
Number of Figures: 4
Number of References: 72
Number of words in the Abstract: 244
Number of words in the Introduction: 675
Number of words in the Results: 1947
Number of words in the Discussion: 1036

Non-standard abbreviations:

AVP	arginine vasopressin
BRET	bioluminescence resonance energy transfer
GFP	green fluorescent protein
HEK cells	Human embryonic kidney cells
RlucII	*Renilla reniformis* luciferase
V2R	Vasopressin V2 receptor

Molecular Pharmacology Fast Forward. Published on July 2, 2022 as DOI: 10.1124/molpharm.122.000497
This article has not been copyedited and formatted. The final version may differ from this version.

Abstract

Activation of the G protein-coupled receptors by agonists may result in the activation of one or more G proteins and recruitment of arrestins. The extent of the activation of each of these pathways depends on the intrinsic efficacy of the ligand. Quantification of intrinsic efficacy relative to a reference compound is essential for the development of novel compounds. In the operational model, changes in efficacy can be compensated by changes in the "functional" affinity, resulting in poorly defined values. To separate the effects of ligand affinity from the intrinsic activity of the receptor, we developed a Michaelis-Menten based quantification of G protein activation bias that uses experimentally measured ligand affinities and provides a single measure of ligand efficacy. We used it to evaluate the signalling of a promiscuous model receptor, the Vasopressin V2 receptor (V2R). Using BRET-based biosensors, we show that the V2R engages many different G proteins across all G protein subfamilies in response to its primary endogenous agonist, arginine vasopressin (AVP), including Gs and members of the Gi/o and G12/13 families. These signaling pathways are also activated by the synthetic peptide desmopressin, oxytocin, and the non-mammalian hormone vasotocin. We compared bias quantification using the operational model with Michaelis-Menten based quantification, the latter accurately quantified ligand efficacies despite large difference in ligand affinities. Together, these results showed that V2R is promiscuous in its ability to engage several G proteins and that its' signaling profile is biased by small structural changes in the ligand.

Molecular Pharmacology Fast Forward. Published on July 2, 2022 as DOI: 10.1124/molpharm.122.000497
This article has not been copyedited and formatted. The final version may differ from this version.

Significance statement: By modelling the G protein activation as Michaelis-Menten reaction, we developed a novel way of quantifying signalling bias. V2R activates or at least engages G proteins from all G protein subfamilies, including Gi2, Gz, Gq, G12, and G13. Their relative activation may explain its Gs-independent signalling.

Molecular Pharmacology Fast Forward. Published on July 2, 2022 as DOI: 10.1124/molpharm.122.000497
This article has not been copyedited and formatted. The final version may differ from this version.

Introduction

G protein-coupled receptors (GPCRs) are a family of membrane proteins involved in many physiological processes, including vision, olfaction, taste, hormone regulation, and neurotransmission. Their ligand-binding sites accessible from the extracellular milieu and their impact on intracellular signaling make them prime drug targets (Rask-Andersen et al., 2014). GPCRs translate ligand-binding events into cellular signals via activation of heterotrimeric G proteins and arrestins. Experimental evidence shows that many receptors can activate or engage more than one G protein isoform, not only within a single subfamily but also across the Gs/olf, Gi/o, Gq/11, and G12/13 subfamilies of heterotrimeric G proteins (Ashkenazi et al., 1987; Cotecchia et al., 1990; Crawford et al., 1992; Fargin et al., 1989; Gudermann et al., 1992; Laprairie et al., 2017; Vallar et al., 1990; Van Sande et al., 1990; Zhu et al., 1994). The realization that some ligands can be agonists for one pathway and antagonists for another led to the development of the concept of biased signaling (Azzi et al., 2003; Galandrin et al., 2007; Jarpe et al., 1998; Kenakin and Miller, 2010; MacKinnon et al., 2001; Wei et al., 2003). Such biased ligands are very promising pharmaceuticals because pharmacological benefits are often associated with one pathway while the side-effects are mediated by another (Benredjem et al., 2019; Bohn, 1999; Bohn et al., 2000; Galandrin et al., 2007; Kenakin and Christopoulos, 2013b; Rankovic et al., 2016).

Several approaches to quantify signaling bias have been suggested (reviewed in (Kenakin and Christopoulos, 2013b; Smith et al., 2018)). A widely used approach is based on the Black-Leff operational model that described the ligand binding and effector output of the receptors and provided a framework for the development of quantitative pharmacology (Black and Leff, 1983). It was further developed by Kenakin and Christopoulos (Kenakin and Christopoulos, 2013a; Kenakin et al., 2012) and Rajagopal and Lefkowitz (Rajagopal, 2013; Rajagopal et al., 2011; Stahl et al., 2019). One of the important aspects of this model is its simplicity while capturing essential aspects of the signaling process. On the other hand, it is a heuristic model that links the signaling input to the signaling output without considering the underlying mechanisms.

The vasopressin type 2 receptor (V2R) is a family A GPCR expressed in several tissues(Szczepanska-Sadowska et al., 2021) and is mainly known for its action in the kidney. It mediates the action of the anti-diuretic hormone, arginine-vasopressin (AVP), by promoting the translocation of the water channel aquaporin to the apical membrane of the principal cell of the collecting duct leading to water reabsorption. Although classically known as a Gs-coupled receptor, it has also been proposed to activate Gq (Inoue et al., 2019; Zhu et al., 1994) and was reported to non-productively engage G12 (Okashah et al., 2020) and form non-canonical receptor-Gi-arrestin complexes (Smith et al., 2021). V2R is a target for treating central diabetes insipidus (Moeller et al., 2013; Roth et al., 2014) and polycystic kidney disease (Rinschen et al., 2014; Sparapani et al., 2021).

Molecular Pharmacology Fast Forward. Published on July 2, 2022 as DOI: 10.1124/molpharm.122.000497
This article has not been copyedited and formatted. The final version may differ from this version.

Here, we developed a simple Michaelis-Menten (M-M) approach for quantifying G protein activation that can better separate the effects of ligand affinity vs. potency in calculating the signaling bias. This model accurately describes the behaviour of G protein activation by GPCRs without the need for "functional" affinity, and instead uses K_d values measured in the ligand-binding experiment. The ligand efficacy is reflected by a single parameter, M-M k_{cat}. We show that the V2R can engage many G proteins, including members of the Gq (Gαq, Gα11, Gα14, Gα15) as well as members of the Gi (Gαi1, Gαi2, Gαi3, Gαz) subfamilies. We compared signalling of four closely related natural and synthetic peptide ligands for V2R: AVP, vasotocin, oxytocin, and desmopressin using the developed M-M model as well as the operational model for quantification of bias. Overall, the M-M model robustly reports relative changes in ligand efficacies, and these results suggest that even relatively minor structural changes in the ligand can induce significant signaling bias at the V2R. These findings open the path for discovering biased ligands allowing us to dissect the physiological role of individual pathways.

Molecular Pharmacology Fast Forward. Published on July 2, 2022 as DOI: 10.1124/molpharm.122.000497
This article has not been copyedited and formatted. The final version may differ from this version.

Materials and Methods

Vasopressin V2 receptor ligands

[Arg^8]-Vasopressin (AVP) (Cys-Tyr-Phe-Gln-Asn-Cys-Pro-Arg-Gly-NH_2; disulphide bridge: Cys^1-Cys^6, 1085.25 g/mol), Desmopressin acetate (deamino-Cys-Tyr-Phe-Gln-Asn-Cys-Pro-D-Arg-Gly-NH_2; disulphide bridge: Cys^1-Cys^6, 1069.24 g/mol) and oxytocin acetate (Cys-Tyr-Phe-Gln-Asn-Cys-Pro-Arg-Gly-NH_2; disulphide bridge: Cys^1-Cys^6, 1085.25 g/mol) were purchased from Genemed Synthesis Inc. (San Antonio, TX, USA) and [Arg8]-Vasotocin acetate (Cys-Tyr-Ile-Gln-Asn-Cys-Pro-Arg-Gly-NH_2, disulphide bridge: Cys^1-Cys^6, 1050.22 g/mol) was from Sigma-Aldrich (Ontario, Canada).

Biosensor constructs

Our biosensor measurements are based on BRETassay technology (Dionne et al., 2002). For the plasmids encoding for RlucII-Gα constructs, constructs were prepared using flexible NAAIRS linkers to insert *Renilla* luciferase (RlucII) into the coding sequence of human Gα versions. RlucII was inserted between amino acids Asp^{94} and Phe^{95} of Gαz using NAAIRSTRPRCT and TRPRCTNAAIRS as linkers. The Gαi1, 2 and 3 RlucII fusions contain a duplication of the respective loop where the RlucII was inserted; namely DSA and RLKIDFG for Gαi1, ADPS and NLQIDF for Gαi2, EAA and RLKIDFG for Gαi3, always followed and preceded by NAAIRS, respectively. Insertion positions were Gly^{96}/Asp^{97} for Gαi1, Phe^{95}/Ala^{96} for Gαi2 and Gly^{96}/Glu^{97} for Gαi3. The GαoA construct was described previously (Richard-Lalonde et al., 2013). Gγ1, Gγ2 and Gγ5 were N-terminally tagged with GFP10 as described (Gales et al., 2006) and β-arrestin 1 and 2 were N-terminally fused to RlucII (Perroy et al., 2004). In the protein kinase C (PKC) biosensor, GFP10 was followed by two phospho-sensing domains, FHA1 and FHA2 and two phospho-PKC (pPKC) sequences, the RlucII and the C1b domain from PKCδ. The pPKC sequences can be phosphorylated by natively-expressed PKC, PKCδ then binds DAG, leading to membrane recruitment (Namkung et al., 2018). Activation of the GPCR leads to activation of phospholipase Cβ, followed by accumulation of diacylglycerol (DAG) which activates PKC. The PKC natively expressed in HEK293 cells phosphorylates pPKC1 and 2 domains of the PKC biosensor which causes a conformational change and BRET increase. Through the C1b domain of PKCδ, the sensor is recruited to DAG in the plasma membrane.

Cell culture and transfection

Human embryonic kidney (HEK) 293SL cells were transiently co-transfected with Flag-V2R, different RlucII-Gα variants, Gβ1 and GFP10-Gγ1 for G protein activation measurements and with Flag-V2R, RlucII-β-arrestin1 or 2 and CAAX-GFP10 for β-arrestin recruitment

Molecular Pharmacology Fast Forward. Published on July 2, 2022 as DOI: 10.1124/molpharm.122.000497
This article has not been copyedited and formatted. The final version may differ from this version.

measurements. For Protein kinase C (PKC) activation, HEK293 ΔGq/11/12/13 cells were transiently co-transfected with Flag-V2R and unimolecular PKC biosensor for controls and with Flag-V2R, unimolecular PKC biosensor and either Gq, G11, G14 or G15 for activation experiments. The HEK293 ΔGq/11/12/13 cells were obtained by CRISPR-Cas9 technology (Inoue et al., 2019). Linear 25 kDa polyethyleneimine (PEI) (Polysciences Inc.) was prepared in phosphate-buffered saline (PBS) (Multicell) (PEI:DNA ratio 3:1). Per 0.24 million HEK293SL cells, 1 µg DNA was used. The cells were seeded into white Cellstar® PS 96-well cell culture plates (Greiner Bio-One, Germany) at a density of 20,000 cells per well and grown for 48 h at 37°C with 5% CO_2.

Biosensor measurements

48 h after transfection the 96-well plates were washed with 200 µl PBS/well and 90 µl of Tyrode's buffer (NaCl 137 mM, KCl 0.9 mM, $MgCl_2$ 1 mM, $NaHCO_3$ 11.9 mM, NaH_2PO_4 3.6 mM, Hepes 25 mM, glucose 5.5 mM, $CaCl_2$ 1 mM pH 7.4) were added and the cells were stored at 37°C with 5% CO_2 for 2 h prior to the measurement. For the measurement, the plates are incubated with 10 µl ligand or vehicle per well for 5 min at varying concentrations, then 10 µl coelenterazine 400a (also known as DeepBlueC™) 2.5 µM final were added. After further 5 min of incubation, luminescence and GFP10 counts were measured at 410 and 515 nm, respectively, in a Synergy Neo (Biotek) plate reader using 0.4 s integration time.

Preparation of ligands

All ligands were prepared in 0.1% (w/v) BSA, stock solutions were stored at -20°C while dilutions for the experiments were stored at 4°C. All ligand dilutions for experiments were used within 4 days of preparation.

Michaelis-Menten based description of the G protein activation by a GPCR

In the enzymatic model of GPCR activity, the G protein activation is catalysed by the receptor and is dependent on the agonist binding (Roberts and Waelbroeck, 2004; Waelbroeck et al., 1997). The concentration of the active agonist-bound receptor $R(L)$ is described by a binding isotherm:

$$R(L) = \frac{R_{tot} \cdot L}{K_d + L} \qquad \textit{(Eq. 1)}$$

where R_{tot} is the total concentration of the receptor, L is ligand concentration and K_d is the ligand dissociation constant.

A minimal system considers the formation of product (P, activated G protein, Gα-GTP) as a function of agonist-bound receptor concentration $R(L)$, that is described by the Eq. *1* above, its

Molecular Pharmacology Fast Forward. Published on July 2, 2022 as DOI: 10.1124/molpharm.122.000497
This article has not been copyedited and formatted. The final version may differ from this version.

catalytic activity rate constant k_{cat}, as well as the Michaelis constant K_m for the G protein–receptor interaction. The rate of deactivation of the activated G protein (P) into inactive G protein (S) depends on the concentration of product and the hydrolysis rate constant k_h of GTP to GDP at the Gα subunit.

$$\frac{d[\mathrm{P}]}{dt} = \frac{R(L)\cdot k_{cat}\cdot[\mathrm{S}]}{K_m+[\mathrm{S}]} - k_h\cdot[\mathrm{P}] \quad \textbf{(Eq. 2)}$$

Considering the deactivation of the active G protein via GTP hydrolysis is an important feature of this model as it determines the concentration of the activated G protein.

At steady-state conditions there is an analytical solution yielding the concentration of activated G protein [P] as a function of the total (i.e., inactive and active combined) concentration of the G protein, S_0.

$$[\mathrm{P}] = S_0 - \frac{-\left(\frac{R(L)k_{cat}}{k_h} - S_0 + K_m\right) + \sqrt{\left(\frac{R(L)k_{cat}}{k_h} - S_0 + K_m\right)^2 + 4K_m S_0}}{2} \quad \textit{(Eq. 3)}$$

From the mathematical point of view, what matters for the steady-state solution is the apparent catalytic activity of the receptor–ligand complex in activating a G protein in a given system:

$$A_{cat} = R(L)\cdot\frac{k_{cat}}{k_h} \textit{ (Eq. 4)}$$

where $R(L)$ and k_{cat} depend on the ligand affinity and concentration as well as the ligand signaling properties while k_h depends on the G protein and other system parameters.

Subsequently, the Eq. 3 could be simplified to

$$[\mathrm{P}] = S_0 - \frac{-(A_{cat} - S_0 + K_m) + \sqrt{(A_{cat} - S_0 + K_m)^2 + 4K_m S_0}}{2} \quad \textit{(Eq. 5)}$$

Correspondingly, the steady-state bias factor between two ligands for a given system can be expressed as

$$B_{mm} = \frac{k_{cat}(ligand)}{k_{cat}(reference\ ligand)} = \frac{A_{cat}(ligand)}{A_{cat}(reference\ ligand)} \textit{ (Eq. 6)}$$

at the concentration of the ligand that results in the same occupancy of the receptor.

While in our experiments the values of S_0 and K_m are not known, it is their value relative to the A_{cat} that would define the shape of the response curve. Therefore, for data fitting purposes we set their values to 1 and only interpret changes relative to the reference ligand.

The concentration-response curves of biosensor responses were fitted to the following equation:

Molecular Pharmacology Fast Forward. Published on July 2, 2022 as DOI: 10.1124/molpharm.122.000497
This article has not been copyedited and formatted. The final version may differ from this version.

$$F(L) = \frac{F_1[P]}{S_0} + \frac{F_0(S_0 - [P])}{S_0} \qquad (Eq.\ 7)$$

Where [P] was calculated based on *Eq. 1* and *Eq. 3*, F_0 and F_1 are the biosensor signal values in the non-activated and activated states, respectively. The data for individual ligands were fitted simultaneously to a MM model described above using the in house DataFitter software (D. Veprintsev, https://github.com/dbv123w/DataFitter). A GraphPad PRISM file containing this model is available for download from https://github.com/dbv123w/GPCR_MM.

Simulations of Michaelis-Menten based description of the G protein activation by a GPCR

All simulations were performed using Cell Designer (Funahashi et al., 2003). The value of the parameters of the system (R_{tot}, k_{cat}, k_h, K_m and S_0) were fixed to 1, while the value of the parameter presented on the y-axis and the ligand concentration were varied.

Data analysis using operational model

Data analysis was done in GraphPad Prism version 6.05 for Windows (GraphPad Software, La Jolla California USA, www.graphpad.com). The statistical significance of G protein activation and β-arrestin recruitment was initially assessed by a one-sample t-test compared to 0 with n=3 (*p<0.05, **p<0.01 and ***p<0.001). For concentration-response curves, all data points were normalised to the maximal response obtained with AVP and expressed as percentage. Values are given ±S.E.M for *n* experiments. Bias factors were calculated according to the operational model (Black and Leff, 1983; Gregory et al., 2010). The final equation used for non-linear curve fitting is:

$$E = basal + \frac{E_m - basal}{1 + \left(\frac{[A]}{10^{\log K_A}} + 1\right)^n}$$

where E is the ligand effect, [A] is the agonist concentration, E_m is the maximal response of the system, basal is the signal in absence of ligand, K_A is the functional equilibrium constant, R is the transduction coefficient $\frac{\tau}{K_A}$ where τ is an index for the efficacy of the agonist and n is the slope (Evans et al., 2011; Kenakin and Christopoulos, 2013b; Kenakin et al., 2012; van der Westhuizen et al., 2014).

Molecular Pharmacology Fast Forward. Published on July 2, 2022 as DOI: 10.1124/molpharm.122.000497
This article has not been copyedited and formatted. The final version may differ from this version.

Results

Analysis of the G protein activation using the Michaelis-Menten formalism

One of the very promising approaches to describe and quantify the activity of GPCRs receptors *in vivo* and in vitro is by the enzymatic model (Roberts and Waelbroeck, 2004; Waelbroeck et al., 1997) and, in its simplified form, by the Michaelis-Menten formalism (Ernst et al., 2007; Maeda et al., 2014). The receptor is considered an enzyme that catalyzes the conversion of substrate to product, i.e., inactive G protein to activated G protein. Therefore, it is important to consider that the activated G protein will be de-activated by auto-hydrolysis of bound GTP to GDP. The use of this model allows obtaining the intrinsic enzymatic activity of the ligand-receptor complex towards a G protein that can be used for the calculations of intrinsic bias factors. To reliably fit concentration-response curves, it is essential to keep the model simple, with a minimal number of parameters. Therefore, the Michaelis-Menten formalism is preferred to the full enzymatic model as it has the same number of parameters as the operational model.

In silico analysis of the Michaelis-Menten model of G protein activation

The first parameter to consider is the concentration of available G protein (S_0). The ability of the G protein to interact with the activated receptors is determined by the second parameter, the Michaelis constant K_m. K_m describes the concentration of G protein at which the G protein activation by the receptor is half-maximal. Third, the number of active receptors is a combination of the receptor number and activity ($R_{tot} \cdot k_{cat}$). High activity can compensate for low receptor numbers and vice versa. The final parameter is k_h, the rate of hydrolysis of GTP to GDP at the G protein, which returns the G protein to its inactive state. The mathematical description of this model is included in the Methods section (Eq. *1-3*). To explore the model and the impact of parameters' variations, we modeled effects of receptor activity, G protein deactivation, G protein concentration, and the K_m of the G proteins towards receptor on the observed activation of the G proteins and, correspondingly, biosensor responses (Fig. 1 and 2). The system needs sufficient G protein (comparable to the K_m value or above) for the G protein activation to take place. However, further increase in the G protein concentration does not increase the potency of the response (i.e., left shift of the curve) as the response (under simulation conditions, see Methods) follows the ligand-binding curve (Fig. 2). Correspondingly, K_m should be comparable or lower than the concentration of the G protein for the activation to happen (Fig. 2). The system response is far more sensitive to changes in the catalytic activity of the activated receptor (k_{cat}) and the rate of the G protein deactivation (k_h) than to changes in K_m or total G protein concentration S_0. The more active the receptor is, the fewer active receptor molecules are needed to reach 50% of the response, leading to a left shift of the activation curve relative to the ligand binding. Therefore, the model captures the classical "receptor reserve" concept (Kenakin, 2014). In contrast, an

Molecular Pharmacology Fast Forward. Published on July 2, 2022 as DOI: 10.1124/molpharm.122.000497
This article has not been copyedited and formatted. The final version may differ from this version.

increase in the rate of G protein deactivation k_h (Fig. 3) directly opposes the activity of the receptor (k_{cat}). To test and compare our newly developed model, we evaluated the signalling of a promiscuous GPCR, the Vasopressin V2 receptor, for four peptide ligands.

Vasopressin V2 receptor recruits members of all G protein families and both β-arrestins

We used biosensors based on bioluminescence resonance energy transfer (BRET) to study the engagement of different G proteins. For the heterotrimer Gαβγ biosensor, the Gα subunit was tagged with luciferase (RlucII) (Breton et al., 2010; Gales et al., 2006; Schonegge et al., 2017), and the Gγ subunit was tagged with GFP10 (Fig. 3A, Methods). We measured the ligand-mediated ΔBRET for different Gα proteins. V2R was able to engage Gαs, Gαi1, Gαi2, Gαi3, Gαz, Gαq, Gα12 and Gα13 to different extents in response to the natural ligand, AVP, but failed to recruit or activate GαoA and GαoB (Fig. 3B). These data indicate that V2R can engage a broad panel of G protein belonging to all the subfamilies, beyond the previously reported Gs and Gq (Inoue et al., 2019; Zhu et al., 1994). To further explore V2R Gq activation, we used a protein kinase C (PKC) biosensor (Namkung et al., 2018) in Gq/11/12/13 knock-out cells (Gq-KO) (Inoue et al., 2019), supplemented with the individual Gα subunits. This biosensor detects the phosphorylation-induced association of forkhead-associated domains selectively binding to PKC-phosphorylated sites (Fig. 3C). Upon addition of AVP, no PKC activation could be detected in Gq-KO cells. However, significant PKC activation was observed upon complementation with Gαq, Gα11, Gα14, or Gα15 (Fig. 3D). The specific activation of PKC through co-transfected Gq family members shows that V2R not only couples to but also activates all Gq/11 family members. In addition, we tested G protein activation in combination with three different Gγ subunits: Gγ1, Gγ2, and Gγ5 (Fig. 3E) for G proteins where we detected engagement, except for the canonically activated Gs. AVP led to a decrease in BRET signal for all the Gγ tested for the Gi and Gq family members. For G12, although a robust BRET decrease was observed with Gγ1, BRET signal increases were observed for Gγ2 and Gγ5. This observation may indicate a difference in the interaction of V2R with Gα12 compared to other Gα subunits in agreement with a recent study reporting the formation of unproductive V2R-Gα12 complexes(Okashah et al., 2020). For G13, BRET decreases were observed for Gγ1 and Gγ2 but not for Gγ5, pointing to a different generalized type of interaction for the G12/13 family members. In addition, we measured β-arrestin recruitment using an enhanced bystander BRET (ebBRET)-based biosensor that uses RlucII-β-arrestin 1 or 2 and a *Renilla* GFP (rGFP)-tagged CAAX box domain from KRas, which is inserted into the membrane (Fig. 3F) (Namkung et al., 2016). V2R recruited both β-arrestins to the same extent (Fig. 3G) at saturating concentrations of AVP, consistent with published data (Oakley et al., 2000).

Molecular Pharmacology Fast Forward. Published on July 2, 2022 as DOI: 10.1124/molpharm.122.000497
This article has not been copyedited and formatted. The final version may differ from this version.

Slight differences in peptide ligand sequences give rise to functional selectivity

To determine signaling bias among peptide ligands, we compared AVP to the clinically used analog desmopressin, the non-mammalian analog vasotocin, and the low potency natural agonist oxytocin. The nonapeptides contain a disulfide bridge and differ in either one or two amino acids (Fig. 4A). Desmopressin contains deamino-Cys instead of Cys at position 1 and D-Arg instead of Arg at position 8. In vasotocin, Leu is replaced with Ile at position 3, a change also found in oxytocin. In addition, oxytocin contains a Leu at position 8 instead of the Arg present in AVP. We tested the effect of these four ligands on G protein engagement, protein kinase C activation through Gαq family members and β-arrestin 1/2 recruitment. We measured concentration-response curves to determine efficacy and potency (pEC50) (Fig. 4B). In our experiments, all ligands were full agonists or strong partial agonists for β-arrestin recruitment and G protein engagement (for statistical evaluation, see Table S1). However, the potencies (pEC50) differed by almost 2.5 orders of magnitude between AVP and oxytocin (Table 1), which agrees with previously measured radio-ligand binding data. (Chini et al., 1995) (Table 2). The efficacies and potencies of the tested ligands were similar for Gq activation tested using the PKC biosensor versus direct activation with the Gα-Gγ biosensor (Table 1). All the pathways followed the affinity rank order except for Gz, G12, and G13. For G13, AVP and desmopressin were equipotent, and for G12 and Gz, AVP, desmopressin and vasotocin were equipotent. In addition, oxytocin showed a preference towards G protein engagement, with a lower potency for recruitment of β-arrestin than for G proteins. None of the ligands showed a preference for one of the β-arrestins.

To quantify ligand biases, we calculated transduction coefficients ($\log(\tau/K_A)$ values) according to the operational model of agonism (Fig. 4C) (Black and Leff, 1983; Black et al., 1985; Kenakin et al., 2012). AVP was chosen as the reference agonist (Table 3). The choice of a reference agonist is necessary to eliminate observational and system bias (Kenakin and Christopoulos, 2013b). The signaling responses to desmopressin and vasotocin were reduced by a factor of 3-5 except for G12 and Gz. For oxytocin, the responses for all pathways, including Gz and G12, was reduced by about a factor of 100. Comparison of the ability of the V2R to activate G proteins (Fig. 4) relative to the reported affinity (Table 2) does not indicate that oxytocin is a particularly weak agonist compared to other peptides. Considering that all peptides elicited the full amplitude of the biosensor response, the τ should be relatively large (i.e., >10), and the difference between the receptor-ligand complex formation and the effector activation response curve should be separated by at least a log unit (Black et al., 1985). On the other hand, the $\Delta\log(\tau/K_A)$ values were significantly reduced for the lower-affinity ligands, implying a potential overestimation of the K_A value that reflects the affinity of the agonist for the "active" state of the receptor. Both τ and K_A are estimated by fitting the same concentration-response curves, which significantly increases the uncertainty of their evaluation. An alternative application of the Black-Leff

Molecular Pharmacology Fast Forward. Published on July 2, 2022 as DOI: 10.1124/molpharm.122.000497
This article has not been copyedited and formatted. The final version may differ from this version.

operational model has also been used for evaluating signaling bias (Rajagopal, 2013; Rajagopal et al., 2011), where the value of K_A is derived from ligand binding experiments. This prompted us to develop alternative metrics that would link the bias calculations to the experimentally measured ligand affinity and report changes in receptor activity towards a particular effector at an equal level of receptor saturation by the ligand.

Application of Michaelis-Menten model to the experimental data

To apply the developed M-M model to available experimental data, further assumptions need to be made. The rate of the G protein deactivation (specific for a G protein type) is determined by the "system" (the cells used for the experiments) and can be assumed to be constant. While we anticipate the K_m values for a given effector to be affected by the ligand, it should still be comparable to the G protein concentration. It does not introduce significant error in the system. Therefore, $\underline{k}_{cat}$ is the only significant parameter that determines the system's behavior, all other parameters can be kept constant. The values are set to one in arbitrary units for the purpose of the fit and are canceled out by normalization. Normalization of the obtained k_{cat} to that of a reference compound allows us to define a Michaelis-Menten bias factor B_{mm}, where

$B_{mm} = k_{cat}(\text{ligand})/k_{cat}(\text{reference ligand})$

The concentration-response curves were fitted directly considering the reported K_d values (Chini et al., 1995) (see Methods). We have applied this model to the Gαβγ BRET-based biosensor data (Fig. 4B).

Comparison of Michaelis-Menten and operational models

The most noticeable difference to the bias factors calculated using the operational model is that the intrinsic activity and B_{mm} bias factors of oxytocin are comparable to those of other peptides (Fig. 4D). This mirrors direct observations of the oxytocin activity as presented in Fig. 4B. As the affinity of the ligand does not affect the calculated k_{cat} or B_{mm}, the differences in the efficacy of the V2R towards G proteins in response to binding of diverse ligands are more accentuated. Oxytocin shows a significantly reduced ability to promote V2R-mediated activation of Gs and Gi2 compared to AVP and other peptides. Compared to AVP, all tested peptides have an increased ability to promote G12 engagement but reduced ability to activate Gq. This parallels the analysis done using the operational model (Table 4). The results strongly suggest that ligands can readily bias V2R signaling, and even relatively small structural differences in peptide ligand sequence seem to be sufficient to induce this effect.

Molecular Pharmacology Fast Forward. Published on July 2, 2022 as DOI: 10.1124/molpharm.122.000497
This article has not been copyedited and formatted. The final version may differ from this version.

Discussion

Michaelis-Menten quantification of receptor activity

Previous work has shown the applicability of the enzymatic model of GPCR activity (Roberts and Waelbroeck, 2004; Waelbroeck et al., 1997). Kenakin and Christopoulos have commented on the apparent similarity between the operational model and the Michaelis-Menten equation (Kenakin and Christopoulos, 2013a). However, despite the apparent mathematical similarity, the actual solution for the steady-state concentration of activated G protein is rather different (see Methods). Here we showed that M-M model describes the activation of G proteins as a function of ligand concentration rather well. The reported efficacy parameter k_{cat} has the same meaning as τ in the operational model, and the ratio of these parameters for two ligands activating the same pathway is a measure of ligand bias. The use of the experimentally reported ligand affinity simplifies the analysis and improves the robustness of the k_{cat} estimation from the concentration-response curves.

It should also be noted that the simplified Michaelis-Menten model presented here can describe G protein activation but not β-arrestin recruitment due to the underlying nature of the two processes. First, it assumes that the number of receptor molecules is small compared to the number of G protein molecules. For most receptors, even in the over-expressed systems, this condition is very likely to be satisfied. Secondly, it also assumes that the activation of the G proteins is non-reversible during the enzymatic step. Given the very high affinity of GTP for the G protein compared to GDP while their concentrations are comparable (0.1-0.5 mM) (Traut, 1994) and the slow hydrolysis-driven deactivation of G proteins, this condition is also very likely to be satisfied. While RGS proteins may control the rate of GTP hydrolysis of Gi and Gq proteins, they only interact with active forms of Gα subunits after they have dissociated from Gβγ after the activation step (Tesmer, 2009). Thirdly, it is important to consider the differences between the signals reported by the G protein, PKC, and arrestin biosensors. While G proteins are activated directly by the receptors, PKC is activated by several nested enzymatic cycles, requiring a much more complicated model incorporating several Michaelis-Menten reactions.

Arrestin biosensors report the formation of the receptor-arrestin complex with a 1:1 stoichiometry. Since this is a binding rather than an enzymatic event, it would not be appropriate to analyze the results obtained with these arrestin-recruitment biosensors using Michaelis-Menten formalism. Recent reports suggested that arrestins may be activated and dissociate from the receptors while maintaining the active state (Eichel et al., 2018). If this is indeed the case, it may be possible to extend the use of this model to arrestins. However, different biosensors directly reporting on the activation status of arrestin would have to be used (Charest et al., 2005; Lee et al., 2016; Nuber et al., 2016; Zimmerman et al., 2012). One of the important advantages of the Michaelis-Menten formalism presented here is that it can be extended to describe the

Molecular Pharmacology Fast Forward. Published on July 2, 2022 as DOI: 10.1124/molpharm.122.000497
This article has not been copyedited and formatted. The final version may differ from this version.

kinetics of signaling processes and not only the steady-state equilibria. The appreciation that signaling may not be an equilibrium process and the importance of considering the kinetics in quantifying bias is growing (Klein Herenbrink et al., 2016). We expect that the application of Michaelis-Menten formalism would be of great advantage in kinetic bias quantification, to study how signaling bias may affect acute, short term signaling events (e.g., cAMP concentration) versus long term (e.g., changes in gene transcription) effects of GPCR activation.

V2R promiscuity

We observed that the V2R promiscuously engaged G proteins from all subfamilies. Although Gs and Gq coupling was previously discussed (Inoue et al., 2019; Zhu et al., 1994) and non-productive G12 engagement was recently described, Gi coupling has only been implied in previous studies (Okashah et al., 2020). Our PKC activation data point towards the activation of Gq by the V2R. All other G proteins (Gi2, Gz, G12, G13) were at least engaged.

The biological significance of this promiscuity of engagement is beyond the scope of the present study. According to the Protein Atlas (www.proteinatlas.org) (Uhlen et al., 2015), V2R is expressed in practically all tissues, except for the brain and the liver. Most Gα isoforms are also expressed in all tissues. Therefore, V2R can interact with all G proteins in native tissues, suggesting that its promiscuity may be biologically relevant. Dual Gs/Gi coupling has been reported for other receptors such as the β2- and the β1-adrenergic receptors (Lukasheva et al., 2020; Xiao et al., 1995); one possible rationale for activation of both Gs and Gi/o proteins is to fine-tune the cAMP response (Stefan et al., 2011). However, this does not account for the activation of Gq/11 and recruitment of G12/13 families. Another possibility is that the biological process triggered by the V2R may have to be mediated by a combination of signaling pathways. Recent medium- and large-scale profiling experiments confirmed that promiscuity is relatively common among GPCRs (Avet et al., 2022; Inoue et al., 2019; Okashah et al., 2019).

Ligand-induced signaling bias

Both the affinity of peptides for V2R and their signaling properties are affected by amino acid substitutions (Table 2). Any modification of AVP tested resulted in decreased ability to activate Gq and increased ability to engage G12 (Fig. S1). Oxytocin's double substitution reduced the ability of V2R to engage Gs and Gi proteins relative to the other G protein subtypes engaged by the receptor.

Similarly, the substitution of the L-Arg for D-Arg in desmopressin may be responsible for the reduced Gi/Gq engagement. This suggests that there are signaling bias hotspots in the ligand-

Molecular Pharmacology Fast Forward. Published on July 2, 2022 as DOI: 10.1124/molpharm.122.000497
This article has not been copyedited and formatted. The final version may differ from this version.

binding pocket. Similar observations were reported for oxytocin receptors where slight oxytocin peptide modifications resulted in different signaling preferences (Busnelli et al., 2012). The peptide ligands of angiotensin receptor and chemokine receptors are another example (Ahn et al., 2004; Namkung et al., 2018; Wei et al., 2003)(reviewed in (Steen et al., 2014)). It is tempting to speculate that receptor-peptide pairs may have co-evolved as a mechanism to change the activity of ancestral receptors.

Conclusions

The proposed Michaelis-Menten approach can be readily applied to existing concentration-response curves and provides robust estimates of intrinsic ligand efficacy. Its application can help to deconvolute functional differences between ligands and contribute to drug development. We hope it will become a valuable analysis approach in the toolbox of modern pharmacology.

Acknowledgments

We thank Steven Charlton and Nicholas Holliday for valuable discussions.

Authorship contributions

Conducted experiments: FMH, BP, JZ, BB, CLG
Contributed new reagents or analytic tools: AR, AI, MB, DBV
Performed data analysis: FMH, BP, AR, DBV
Wrote or contributed to the writing of the manuscript: FMH, BP, DM, MB, DBV

Molecular Pharmacology Fast Forward. Published on July 2, 2022 as DOI: 10.1124/molpharm.122.000497
This article has not been copyedited and formatted. The final version may differ from this version.

References:

Ahn S, Shenoy SK, Wei H and Lefkowitz RJ (2004) Differential kinetic and spatial patterns of beta-arrestin and G protein-mediated ERK activation by the angiotensin II receptor. *J Biol Chem* **279**(34): 35518-35525.

Ashkenazi A, Winslow J, Peralta E, Peterson G, Schimerlik M, Capon D and Ramachandran J (1987) An M2 muscarinic receptor subtype coupled to both adenylyl cyclase and phosphoinositide turnover. *Science* **238**(4827): 672-675.

Avet C, Mancini A, Breton B, Le Gouill C, Hauser AS, Normand C, Kobayashi H, Gross F, Hogue M, Lukasheva V, St-Onge S, Carrier M, Heroux M, Morissette S, Fauman EB, Fortin JP, Schann S, Leroy X, Gloriam DE and Bouvier M (2022) Effector membrane translocation biosensors reveal G protein and betaarrestin coupling profiles of 100 therapeutically relevant GPCRs. *Elife* **11**.

Azzi M, Charest PG, Angers S, Rousseau G, Kohout T, Bouvier M and Piñeyro G (2003) Beta-arrestin-mediated activation of MAPK by inverse agonists reveals distinct active conformations for G protein-coupled receptors. *Proc Natl Acad Sci USA* **100**(20): 11406-11411.

Benredjem B, Gallion J, Pelletier D, Dallaire P, Charbonneau J, Cawkill D, Nagi K, Gosink M, Lukasheva V, Jenkinson S, Ren Y, Somps C, Murat B, Van Der Westhuizen E, Le Gouill C, Lichtarge O, Schmidt A, Bouvier M and Pineyro G (2019) Exploring use of unsupervised clustering to associate signaling profiles of GPCR ligands to clinical response. *Nat Commun* **10**(1).

Black JW and Leff P (1983) Operational models of pharmacological agonism. *Proceedings of the Royal Society of London Series B, Biological sciences* **220**(1219): 141-162.

Black JW, Leff P, Shankley NP and Wood J (1985) An operational model of pharmacological agonism: the effect of E/[A] curve shape on agonist dissociation constant estimation. *Br J Pharmacol* **84**(2): 561-571.

Bohn LM (1999) Enhanced Morphine Analgesia in Mice Lacking -Arrestin 2 . *Science* **286**(5449): 2495-2498.

Bohn LM, Gainetdinov RR, Lin FT, Lefkowitz RJ and Caron MG (2000) Mu-opioid receptor desensitization by beta-arrestin-2 determines morphine tolerance but not dependence. *Nature* **408**(6813): 720-723.

Breton B, Sauvageau É, Zhou J, Bonin H, Le Gouill C and Bouvier M (2010) Multiplexing of Multicolor Bioluminescence Resonance Energy Transfer. *Biophysical Journal* **99**(12): 4037-4046.

Busnelli M, Sauliere A, Manning M, Bouvier M, Gales C and Chini B (2012) Functional selective oxytocin-derived agonists discriminate between individual G protein family subtypes. *J Biol Chem* **287**(6): 3617-3629.

Charest PG, Terrillon S and Bouvier M (2005) Monitoring agonist-promoted conformational changes of beta-arrestin in living cells by intramolecular BRET. *EMBO Rep* **6**(4): 334-340.

Chini B, Mouillac B, Ala Y, Balestre MN, Trumpp-Kallmeyer S, Hoflack J, Elands J, Hibert M, Manning M, Jard S and et al. (1995) Tyr115 is the key residue for determining agonist selectivity in the V1a vasopressin receptor. *EMBO J* **14**(10): 2176-2182.

Cotecchia S, Kobilka BK, Daniel KW, Nolan RD, Lapetina EY, Caron MG, Lefkowitz RJ and Regan JW (1990) Multiple second messenger pathways of alpha-adrenergic receptor subtypes expressed in eukaryotic cells. *J Biol Chem* **265**(1): 63-69.

Crawford KW, Frey EA and Cote TE (1992) Angiotensin II receptor recognized by DuP753 regulates two distinct guanine nucleotide-binding protein signaling pathways. *Mol Pharmacol* **41**(1): 154-162.

Dionne P, Caron M, Labonté A, Carter-Allen K, Houle B, Joly E, Taylor SC and L. M (2002) BRET2: efficient energy transfer from Renilla luciferase to GFP2 to measure protein–protein interactions and intracellular signaling events in live cells. , in *Luminescence biotechnology: instruments and*

applications (van Dyke K, van Dyke C and Woodfork K eds) pp 539–555, CRC Press, Boca Raton (FL).

Eichel K, Jullié D, Barsi-Rhyne B, Latorraca NR, Masureel M, Sibarita J-B, Dror RO and von Zastrow M (2018) Catalytic activation of β-arrestin by GPCRs. *Nature* **557**(7705): 381-386.

Ernst OP, Gramse V, Kolbe M, Hofmann KP and Heck M (2007) Monomeric G protein-coupled receptor rhodopsin in solution activates its G protein transducin at the diffusion limit. *Proc Natl Acad Sci U S A* **104**(26): 10859-10864.

Evans BA, Broxton N, Merlin J, Sato M, Hutchinson DS, Christopoulos A and Summers RJ (2011) Quantification of Functional Selectivity at the Human {alpha}1A-Adrenoceptor. *Mol Pharmacol* **79**(2): 298-307.

Fargin A, Raymond JR, Regan JW, Cotecchia S, Lefkowitz RJ and Caron MG (1989) Effector coupling mechanisms of the cloned 5-HT1A receptor. *J Biol Chem* **264**(25): 14848-14852.

Funahashi A, Morohashi M, Kitano H and Tanimura N (2003) CellDesigner: a process diagram editor for gene-regulatory and biochemical networks. *Biosilico* **1**(5): 159-162.

Galandrin S, Oligny-Longpre G and Bouvier M (2007) The evasive nature of drug efficacy: implications for drug discovery. *Trends Pharmacol Sci* **28**(8): 423-430.

Gales C, Van Durm JJ, Schaak S, Pontier S, Percherancier Y, Audet M, Paris H and Bouvier M (2006) Probing the activation-promoted structural rearrangements in preassembled receptor-G protein complexes. *Nature structural & molecular biology* **13**(9): 778-786.

Gudermann T, Birnbaumer M and Birnbaumer L (1992) Evidence for dual coupling of the murine luteinizing hormone receptor to adenylyl cyclase and phosphoinositide breakdown and Ca2+ mobilization. Studies with the cloned murine luteinizing hormone receptor expressed in L cells. *J Biol Chem* **267**(7): 4479-4488.

Inoue A, Raimondi F, Kadji FMN, Singh G, Kishi T, Uwamizu A, Ono Y, Shinjo Y, Ishida S, Arang N, Kawakami K, Gutkind JS, Aoki J and Russell RB (2019) Illuminating G-Protein-Coupling Selectivity of GPCRs. *Cell*.

Jarpe MB, Knall C, Mitchell FM, Buhl AM, Duzic E and Johnson GL (1998) [D-Arg1,D-Phe5,D-Trp7,9,Leu11]Substance P acts as a biased agonist toward neuropeptide and chemokine receptors. *J Biol Chem* **273**(5): 3097-3104.

Kenakin T and Christopoulos A (2013a) Measurements of ligand bias and functional affinity. *Nat Rev Drug Discov* **12**(6): 483-483.

Kenakin T and Christopoulos A (2013b) Signalling bias in new drug discovery: detection, quantification and therapeutic impact. *Nature reviews Drug discovery* **12**(3): 205-216.

Kenakin T and Miller LJ (2010) Seven transmembrane receptors as shapeshifting proteins: the impact of allosteric modulation and functional selectivity on new drug discovery. *Pharmacological reviews* **62**(2): 265-304.

Kenakin T, Watson C, Muniz-Medina V, Christopoulos A and Novick S (2012) A Simple Method for Quantifying Functional Selectivity and Agonist Bias. *ACS chemical neuroscience* **3**(3): 193-203.

Kenakin TP (2014) *A pharmacology primer : techniques for more effective and strategic drug discovery*. Fourth edition. ed. Elsevier Academic Press, Amsterdam ; Boston.

Klein Herenbrink C, Sykes DA, Donthamsetti P, Canals M, Coudrat T, Shonberg J, Scammells PJ, Capuano B, Sexton PM, Charlton SJ, Javitch JA, Christopoulos A and Lane JR (2016) The role of kinetic context in apparent biased agonism at GPCRs. *Nat Commun* **7**(1).

Laprairie RB, Stahl EL and Bohn LM (2017) Approaches to Assess Biased Signaling at the CB1R Receptor. *Methods Enzymol* **593**: 259-279.

Lee MH, Appleton KM, Strungs EG, Kwon JY, Morinelli TA, Peterson YK, Laporte SA and Luttrell LM (2016) The conformational signature of beta-arrestin2 predicts its trafficking and signalling functions. *Nature* **531**(7596): 665-668.

Lukasheva V, Devost D, Le Gouill C, Namkung Y, Martin RD, Longpré J-M, Amraei M, Shinjo Y, Hogue M, Lagacé M, Breton B, Aoki J, Tanny JC, Laporte SA, Pineyro G, Inoue A, Bouvier M and Hébert TE (2020) Signal profiling of the β1AR reveals coupling to novel signalling pathways and distinct phenotypic responses mediated by β1AR and β2AR. *Scientific reports* **10**(1).

MacKinnon AC, Waters C, Jodrell D, Haslett C and Sethi T (2001) Bombesin and substance P analogues differentially regulate G-protein coupling to the bombesin receptor. Direct evidence for biased agonism. *J Biol Chem* **276**(30): 28083-28091.

Maeda S, Sun D, Singhal A, Foggetta M, Schmid G, Standfuss J, Hennig M, Dawson RJ, Veprintsev DB and Schertler GF (2014) Crystallization scale preparation of a stable GPCR signaling complex between constitutively active rhodopsin and G-protein. *PLoS ONE* **9**(6): e98714.

Moeller HB, Rittig S and Fenton RA (2013) Nephrogenic Diabetes Insipidus: Essential Insights into the Molecular Background and Potential Therapies for Treatment. *Endocrine Reviews* **34**(2): 278-301.

Namkung Y, Le Gouill C, Lukashova V, Kobayashi H, Hogue M, Khoury E, Song M, Bouvier M and Laporte SA (2016) Monitoring G protein-coupled receptor and beta-arrestin trafficking in live cells using enhanced bystander BRET. *Nat Commun* **7**: 12178.

Namkung Y, LeGouill C, Kumar S, Cao Y, Teixeira LB, Lukasheva V, Giubilaro J, Simões SC, Longpré J-M, Devost D, Hébert TE, Piñeyro G, Leduc R, Costa-Neto CM, Bouvier M and Laporte SA (2018) Functional selectivity profiling of the angiotensin II type 1 receptor using pathway-wide BRET signaling sensors. *Science Signaling* **11**(559).

Nuber S, Zabel U, Lorenz K, Nuber A, Milligan G, Tobin AB, Lohse MJ and Hoffmann C (2016) beta-Arrestin biosensors reveal a rapid, receptor-dependent activation/deactivation cycle. *Nature* **531**(7596): 661-664.

Oakley RH, Laporte SA, Holt JA, Caron MG and Barak LS (2000) Differential affinities of visual arrestin, beta arrestin1, and beta arrestin2 for G protein-coupled receptors delineate two major classes of receptors. *J Biol Chem* **275**(22): 17201-17210.

Okashah N, Wan Q, Ghosh S, Sandhu M, Inoue A, Vaidehi N and Lambert NA (2019) Variable G protein determinants of GPCR coupling selectivity. *Proceedings of the National Academy of Sciences*.

Okashah N, Wright SC, Kawakami K, Mathiasen S, Zhou J, Lu S, Javitch JA, Inoue A, Bouvier M and Lambert NA (2020) Agonist-induced formation of unproductive receptor-G12 complexes. *Proc Natl Acad Sci U S A*.

Perroy J, Pontier S, Charest PG, Aubry M and Bouvier M (2004) Real-time monitoring of ubiquitination in living cells by BRET. *Nat Methods* **1**(3): 203-208.

Rajagopal S (2013) Quantifying biased agonism: understanding the links between affinity and efficacy. *Nat Rev Drug Discov* **12**(6): 483-483.

Rajagopal S, Ahn S, Rominger DH, Gowen-MacDonald W, Lam CM, DeWire SM, Violin JD and Lefkowitz RJ (2011) Quantifying Ligand Bias at Seven-Transmembrane Receptors. *Molecular Pharmacology* **80**(3): 367-377.

Rankovic Z, Brust TF and Bohn LM (2016) Biased agonism: An emerging paradigm in GPCR drug discovery. *Bioorg Med Chem Lett* **26**(2): 241-250.

Rask-Andersen M, Masuram S and Schiöth HB (2014) The Druggable Genome: Evaluation of Drug Targets in Clinical Trials Suggests Major Shifts in Molecular Class and Indication. *Annual Review of Pharmacology and Toxicology* **54**(1): 9-26.

Richard-Lalonde M, Nagi K, Audet N, Sleno R, Amraei M, Hogue M, Balboni G, Schiller PW, Bouvier M, Hebert TE and Pineyro G (2013) Conformational dynamics of Kir3.1/Kir3.2 channel activation via delta-opioid receptors. *Mol Pharmacol* **83**(2): 416-428.

Rinschen MM, Schermer B and Benzing T (2014) Vasopressin-2 Receptor Signaling and Autosomal Dominant Polycystic Kidney Disease: From Bench to Bedside and Back Again. *Journal of the American Society of Nephrology* **25**(6): 1140-1147.

Roberts DJ and Waelbroeck M (2004) G protein activation by G protein coupled receptors: ternary complex formation or catalyzed reaction? *Biochemical pharmacology* **68**(5): 799-806.

Roth J, Bichet DG, Galiveeti S and Qureshi S (2014) Diabetes Insipidus: Celebrating a Century of Vasopressin Therapy. *Endocrinology* **155**(12): 4605-4621.

Schonegge AM, Gallion J, Picard LP, Wilkins AD, Le Gouill C, Audet M, Stallaert W, Lohse MJ, Kimmel M, Lichtarge O and Bouvier M (2017) Evolutionary action and structural basis of the allosteric switch controlling beta2AR functional selectivity. *Nat Commun* **8**(1): 2169.

Smith JS, Lefkowitz RJ and Rajagopal S (2018) Biased signalling: from simple switches to allosteric microprocessors. *Nature Reviews Drug Discovery* **17**(4): 243-260.

Smith JS, Pack TF, Inoue A, Lee C, Zheng K, Choi I, Eiger DS, Warman A, Xiong X, Ma Z, Viswanathan G, Levitan IM, Rochelle LK, Staus DP, Snyder JC, Kahsai AW, Caron MG and Rajagopal S (2021) Noncanonical scaffolding of Galphai and beta-arrestin by G protein-coupled receptors. *Science* **371**(6534).

Sparapani S, Millet-Boureima C, Oliver J, Mu K, Hadavi P, Kalostian T, Ali N, Avelar CM, Bardies M, Barrow B, Benedikt M, Biancardi G, Bindra R, Bui L, Chihab Z, Cossitt A, Costa J, Daigneault T, Dault J, Davidson I, Dias J, Dufour E, El-Khoury S, Farhangdoost N, Forget A, Fox A, Gebrael M, Gentile MC, Geraci O, Gnanapragasam A, Gomah E, Haber E, Hamel C, Iyanker T, Kalantzis C, Kamali S, Kassardjian E, Kontos HK, Le TBU, LoScerbo D, Low YF, Mac Rae D, Maurer F, Mazhar S, Nguyen A, Nguyen-Duong K, Osborne-Laroche C, Park HW, Parolin E, Paul-Cole K, Peer LS, Philippon M, Plaisir C-A, Porras Marroquin J, Prasad S, Ramsarun R, Razzaq S, Rhainds S, Robin D, Scartozzi R, Singh D, Fard SS, Soroko M, Soroori Motlagh N, Stern K, Toro L, Toure MW, Tran-Huynh S, Trépanier-Chicoine S, Waddingham C, Weekes AJ, Wisniewski A and Gamberi C (2021) The Biology of Vasopressin. *Biomedicines* **9**(1).

Stahl EL, Ehlert FJ and Bohn LM (2019) Quantitating Ligand Bias Using the Competitive Model of Ligand Activity. *Methods in molecular biology (Clifton, NJ* **1957**: 235-247.

Steen A, Larsen O, Thiele S and Rosenkilde MM (2014) Biased and G Protein-Independent Signaling of Chemokine Receptors. *Frontiers in Immunology* **5**.

Stefan E, Malleshaiah MK, Breton B, Ear PH, Bachmann V, Beyermann M, Bouvier M and Michnick SW (2011) PKA regulatory subunits mediate synergy among conserved G-protein-coupled receptor cascades. *Nat Commun* **2**(1).

Szczepanska-Sadowska E, Wsol A, Cudnoch-Jedrzejewska A and Zera T (2021) Complementary Role of Oxytocin and Vasopressin in Cardiovascular Regulation. *International journal of molecular sciences* **22**(21).

Tesmer JJG (2009) Chapter 4 Structure and Function of Regulator of G Protein Signaling Homology Domains, in *Molecular Biology of RGS Proteins* pp 75-113.

Traut TW (1994) Physiological concentrations of purines and pyrimidines. *Molecular and Cellular Biochemistry* **140**(1): 1-22.

Uhlen M, Fagerberg L, Hallstrom BM, Lindskog C, Oksvold P, Mardinoglu A, Sivertsson A, Kampf C, Sjostedt E, Asplund A, Olsson I, Edlund K, Lundberg E, Navani S, Szigyarto CAK, Odeberg J, Djureinovic D, Takanen JO, Hober S, Alm T, Edqvist PH, Berling H, Tegel H, Mulder J, Rockberg J, Nilsson P, Schwenk JM, Hamsten M, von Feilitzen K, Forsberg M, Persson L, Johansson F, Zwahlen M, von Heijne G, Nielsen J and Ponten F (2015) Tissue-based map of the human proteome. *Science* **347**(6220): 1260419-1260419.

Vallar L, Muca C, Magni M, Albert P, Bunzow J, Meldolesi J and Civelli O (1990) Differential coupling of dopaminergic D2 receptors expressed in different cell types. Stimulation of

phosphatidylinositol 4,5-bisphosphate hydrolysis in LtK- fibroblasts, hyperpolarization, and cytosolic-free Ca2+ concentration decrease in GH4C1 cells. *J Biol Chem* **265**(18): 10320-10326.

van der Westhuizen ET, Breton B, Christopoulos A and Bouvier M (2014) Quantification of Ligand Bias for Clinically Relevant β2-Adrenergic Receptor Ligands: Implications for Drug Taxonomy. *Molecular Pharmacology* **85**(3): 492-509.

Van Sande J, Raspe E, Perret J, Lejeune C, Maenhaut C, Vassart G and Dumont JE (1990) Thyrotropin activates both the cyclic AMP and the PIP2 cascades in CHO cells expressing the human cDNA of TSH receptor. *Mol Cell Endocrinol* **74**(1): R1-6.

Waelbroeck M, Boufrahi L and Swillens S (1997) Seven helix receptors are enzymes catalysing G protein activation. What is the agonist Kact? *J Theor Biol* **187**(1): 15-37.

Wei H, Ahn S, Shenoy SK, Karnik SS, Hunyady L, Luttrell LM and Lefkowitz RJ (2003) Independent beta-arrestin 2 and G protein-mediated pathways for angiotensin II activation of extracellular signal-regulated kinases 1 and 2. *Proc Natl Acad Sci U S A* **100**(19): 10782-10787.

Xiao RP, Ji X and Lakatta EG (1995) Functional coupling of the beta 2-adrenoceptor to a pertussis toxin-sensitive G protein in cardiac myocytes. *Mol Pharmacol* **47**(2): 322-329.

Zhu X, Gilbert S, Birnbaumer M and Birnbaumer L (1994) Dual signaling potential is common among Gs-coupled receptors and dependent on receptor density. *Mol Pharmacol* **46**(3): 460-469.

Zimmerman B, Beautrait A, Aguila B, Charles R, Escher E, Claing A, Bouvier M and Laporte SA (2012) Differential beta-arrestin-dependent conformational signaling and cellular responses revealed by angiotensin analogs. *Sci Signal* **5**(221): ra33.

Footnotes

An earlier version of this paper appears in bioRxiv under the doi https://doi.org/10.1101/2021.01.28.427950.

This work was supported by the Swiss National Science Foundation grants 135754 and 159748 to DBV; Swiss National Science Foundation Doc.Mobility P1EZP3_165219 to FMH; and a Foundation grant (# 148431) from the Canadian Institute of Health Research (CIHR) to MB. BP was funded by a Fellowship Award from CIHR (2012-2015) and by a Fellowship Award from Diabetes Canada (2016-2018). MB holds a Canada Research chair in Signal Transduction and Molecular Pharmacology.

MB is the chairman of the Scientific advisory board of Domain Therapeutics, a biotech company to which the BRET-based sensor used in the present study was licensed for commercial use. DBV is a founder of Z7 Biotech, a company specialising in early-stage drug discovery.

Molecular Pharmacology Fast Forward. Published on July 2, 2022 as DOI: 10.1124/molpharm.122.000497
This article has not been copyedited and formatted. The final version may differ from this version.

Figure legends

Figure 1. Activation of the G protein modelled according to the Michaelis-Menten formalism so that G protein activation is half maximal and log(ligand) = 0 refers to the ligand concentration where the concentration of ligand equals K_d. $R_{tot} \cdot k_{cat}$ was modelled as one parameter because a high receptor number (R_{tot}) can compensate for a slow k_{cat} and vice versa. The units are arbitrary. (A) Fraction of active G protein as a function of receptor activity and amount ($R_{tot} \cdot k_{cat}$). (B) examples of individual curves of (A) at several receptor activity levels. (C) Fraction of active G protein as a function of G protein deactivation rate constant k_h. (D) examples of individual curves at different log(k_h) values. Both parameters can result in a shift of the EC50 value as well as the amplitude of the response.

Figure 2. Dependence of G protein activation on total G protein concentration S_0 and the Michaelis constant K_m for G protein–receptor interaction. Either S_0 or K_m was varied, the other parameters were kept constant. In addition, the ligand concentration was varied over three orders of magnitude. (A) The fraction of active G protein is shown as a function of the total amount of G protein in the system (S_0), assuming a K_m value of 1 ($S_0 = K_m$ at log(S_0) = 0). (B) examples of individual curves at several G protein concentrations. (C) The fraction of active G protein as a function of the K_m value between the receptor and the G protein. The lower the value, the stronger the interaction. (D) Examples of the concentration-response curves normalised to the total amount of the G protein in the system.

The EC50 value is not affected by these parameters, but the amplitude is.

Figure 3. Vasopressin V2 receptor activates Gs/olf, Gi/o, Gq/11 and $G_{12/13}$ family proteins and both β-arrestins. **A.** Schematic overview of the direct G protein BRET-based biosensor. Activation of the heterotrimeric G protein by the GPCR leads to dissociation of the Gα from Gβγ and a conformational change in the Gα domain, which result in a decreased BRET signal. **B.** Overview of the arginine-vasopressin (AVP)-induced change in BRET signal for RlucII-tagged Gα subunits and GFP10-tagged Gγ1. **C.** Schematic overview of the protein kinase C (PKC) biosensor. GFP10 is followed by two phospho-sensing domains, FHA1 and FHA2 and two phospho-PKC (pPKC) sequences which can be phosphorylated by natively-expressed PKC, the RlucII and the C1b domain from PKCδ which binds DAG, leading to membrane recruitment. Activation of the GPCR leads to activation of phospholipase Cβ, followed by accumulation of diacylglycerol (DAG) which activates PKC. The PKC natively expressed in HEK293 cells phosphorylates pPKC1 and 2 domains of the PKC biosensor which causes a conformational change and BRET increase. Through the C1b domain of PKCδ, the sensor is recruited to DAG in the plasma membrane. **D.** Overview of the AVP-induced change in BRET signal for the PKC biosensor when different isoforms from the Gq/11 family are cotransfected in Gq/11/12/13 null

Molecular Pharmacology Fast Forward. Published on July 2, 2022 as DOI: 10.1124/molpharm.122.000497
This article has not been copyedited and formatted. The final version may differ from this version.

HEK293 cells. **E.** G protein engagement at saturating AVP concentrations varies with Gγ subunit. Different combinations of Gα and Gγ lead to differing ΔBRET values, numbers in brackets indicate the amino acid where RlucII was fused to Gα. For Gαs, the alternative fusion position after amino acid 67 was used here. **F.** Schematic overview of the β-arrestin recruitment biosensor. Activation of the GPCR leads to phosphorylation of the C-terminus of the receptor followed by recruitment of β-arrestin. **G.** Overview of the AVP-induced change in BRET signal for RlucII-tagged β-arrestins and rGFP-tagged CAAX domain of Kras. The statistical significance was assessed by a one-sample t-test compared to 0 with n=3 (*p<0.05, **p<0.01 and ***p<0.001). Error bars are shown as standard error of mean (SEM).

Figure 4. Biased signalling of V2R peptide ligands. **A.** The peptide ligands differ in only one or two amino acids (marked in red). **B.** Concentration-response curves of biosensor activation for all four peptides, using the heterotrimeric Gαβγ biosensor for G protein engagement, the bystander-BRET β-arrestin biosensor for arrestin recruitment and the PKC biosensor for Gq family activation, labeled '(PKC)'. **C.** Bias as calculated using the operational model for arginine vasopressin (AVP, blue), desmopressin (green), arginine vasotocin (yellow) and oxytocin (red). **D.** The schematic diagram of the Michaelis-Menten model of G protein activation. **E.** The Michaelis-Menten signalling bias. Although the G12 data can be fitted to a M-M model to obtain an apparent Kcat, additional judgement needs to be used to check if this model is applicable.

Molecular Pharmacology Fast Forward. Published on July 2, 2022 as DOI: 10.1124/molpharm.122.000497
This article has not been copyedited and formatted. The final version may differ from this version.

Tables

Table 1. Potencies (pEC50) and agonist-induced maximal response ("amplitude") of G protein, protein kinase C and β-arrestin activation, normalised to the maximal response of Gs. Data are mean ± S.E.M of 2-7 independent experiments done either in triplicates or quadruplicates, see details in Table S1. Numbers in brackets indicate the fusion site of the luciferase in cases where different sensors were used.

pathway	**AVP**		**desmopressin**		**vasotocin**		**oxytocin**	
	pEC50	response	pEC50	response	pEC50	response	pEC50	response
Gs (117)	8.76±0.08	100.9±2.2	8.39±0.14	92.8±4.3	8.08±0.11	85.8±3.4	6.89±0.16	86.8±3.6
Gi2	8.27±0.08	101.6±2.8	7.78±0.14	76.3±4.0	7.58±0.17	93.0±5.8	6.39±0.18	75.5±3.9
Gz	7.98±0.09	98.1±3.7	7.78±0.09	89.7±3.3	7.81±0.10	101.9±3.5	6.31±0.09	93.4±2.8
Gq	8.07±0.06	98.7±2.5	7.66±0.06	85.5±1.9	7.65±0.06	79.7±1.7	6.22±0.07	77.0±1.9
G12	7.79±0.21	86.2±7.2	7.81±0.25	111.4±9.2	7.69±0.22	125.2±10.7	6.10±0.16	118.5±6.4
G13	8.37±0.12	98.7±3.8	8.32±0.13	95.7±3.7	7.92±0.15	89.8±4.1	6.66±0.11	88.0±2.7
PKC (Gq)	8.69±0.07	99. 7±2.3	8.01±0.10	88.8±3.4	8.06±0.16	98.9±5.5	6.25±0.11	84.4±3.6
PKC (G11)	8.79±0.09	99.1±2.9	8.03±0.09	94.4±3.2	8.28±0.12	92.1±3.8	6.48±0.09	97.5±3.0
PKC (G14)	8.63±0.19	97.3±6.6	7.50±0.43	79.4±18.6	7.38±0.24	142.6±14.0	5.83±0.25	96.2±9.6
PKC (G15)	9.26±0.08	99.5±2.2	8.43±0.1	109.2±3.2	8.49±0.09	113.2±3.3	6.77±0.14	98.1±4.4
β-arrestin 1	8.31±0.05	99.2±1.9	7.56±0.05	101.0±2.3	7.54±0.06	96.9±2.2	5.77±0.04	95.0±1.6
β-arrestin 2	8.23±0.05	99.1±2.0	7.50±0.04	98.8±1.7	7.45±0.05	93.9±1.8	5.84±0.04	95.1±1.7

Molecular Pharmacology Fast Forward. Published on July 2, 2022 as DOI: 10.1124/molpharm.122.000497
This article has not been copyedited and formatted. The final version may differ from this version.

Table 2. Dependence of logB_{mm} values on ligand amino-acid sequence, using AVP as the reference peptide. F3L: exchange of a phenylalanine at position 3 for a leucine, R8L: exchange of an arginine at position 8 for a leucine, R(L)8R(D) – exchange of the L- for D-arginine at position 8.

	AVP	desmopressin	vasotocin	oxytocin
deamination	0	1	0	0
F3L	0	0	1	1
R8L	0	0	0	1
R(L)8R(D)	0	1	0	0
log*Ki* **(Chini et al., 1995)**	-8.97	-7.51	-7.6	-5.81
Gs(67) logB_{mm}	0	-0.01	-0.02	-0.17
Gs(117) logB_{mm}	0	0.01	-0.02	-0.16
Gi2 logB_{mm}	0	-0.08	-0.01	-0.16
Gz logB_{mm}	0	-0.03	0.02	-0.05
Gz logB_{mm}	0	-0.09	-0.10	-0.13
G12 logB_{mm}	0	0.11	0.12	0.11
G13 logB_{mm}	0	-0.01	-0.03	-0.06

Molecular Pharmacology Fast Forward. Published on July 2, 2022 as DOI: 10.1124/molpharm.122.000497
This article has not been copyedited and formatted. The final version may differ from this version.

Table 3. Transduction coefficients ($\log(\tau/K_A)$) and $\Delta\log(\tau/K_A)$ with AVP as reference ligand. Data are mean ± S.E.M of 2-7 independent experiments done either in triplicates or quadruplicates.

pathway	AVP	desmopressin		vasotocin		oxytocin	
	$\log(\tau/K_A)$	$\log(\tau/K_A)$	$\Delta\log(\tau/K_A)$	$\log(\tau/K_A)$	$\Delta\log(\tau/K_A)$	$\log(\tau/K_A)$	$\Delta\log(\tau/K_A)$
Gs (67)	8.49±0.20	8.82±0.2	0.33±0.28	8.04±0.21	-0.45±0.29	6.92±0.22	-1.57±0.30
Gs (117)	8.81±0.11	8.20±0.11	-0.61±0.15	7.76±0.11	-1.05±0.16	6.76±0.13	-2.06±0.17
Gi2	8.30±0.14	7.43±0.17	-0.87±0.22	7.54±0.14	-0.76±0.20	6.33±0.21	-1.97±0.25
Gz	7.97±0.11	7.67±0.11	-0.30±0.16	7.80±0.09	-0.18±0.14	6.18±0.11	-1.79±0.15
Gq	8.04±0.04	7.59±0.06	-0.45±0.07	7.66±0.10	-0.38±0.11	6.09±0.08	-1.95±0.11
G12	7.54±0.25	7.88±0.20	0.34±0.32	7.74±0.22	0.20±0.33	6.12±0.18	-1.42±0.31
G13	8.57±0.11	8.56±0.12	-0.01±0.16	7.95±0.12	-0.62±0.16	6.67±0.12	-1.90±0.16
PKC (Gq)	8.68±0.08	7.97±0.11	-0.71±0.13	8.18±0.10	-0.50±0.12	6.19±0.12	-2.49±0.14
PKC (G11)	8.75±0.07	8.04±0.08	-0.71±0.11	8.32±0.09	-0.44±0.11	6.44±0.08	-2.32±0.11
PKC (G14)	8.65±0.33	7.41±0.43	-1.24±0.54	7.51±0.15	-1.14±0.36	6.01±0.36	-2.64±0.49
PKC (G15)	9.16±0.10	8.52±0.09	-0.65±0.13	8.51±0.09	-0.65±0.13	6.64±0.10	-2.53±0.14
β-arrestin 1	8.30±0.05	7.58±0.05	-0.72±0.07	7.50±0.05	-0.80±0.07	5.76±0.05	-2.54±0.07
β-arrestin 2	8.22±0.03	7.52±0.04	-0.69±0.05	7.49±0.05	-0.73±0.05	5.85±0.04	-2.37±0.05

Molecular Pharmacology Fast Forward. Published on July 2, 2022 as DOI: 10.1124/molpharm.122.000497
This article has not been copyedited and formatted. The final version may differ from this version.

Table 4. Comparison of bias between pathways with Gs as a reference (ΔΔlog(τ/KA) values) and bias factors.

pathway	desmopressin		vasotocin		oxytocin	
	ΔΔlog (τ/K_A)	bias factor	ΔΔlog (τ/K_A)	bias factor	ΔΔlog (τ/K_A)	bias factor
Gi2	-0.26±0.27	0.55	0.28±0.26	1.93	0.08±0.31	1.21
Gz	0.32±0.22	2.07	0.87±0.21	7.46	0.27±0.23	1.86
Gq	0.17±0.17	1.47	0.67±0.19	4.69	0.11±0.21	1.28
G12	0.96±0.36	9.06	1.25±0.37	17.58	0.64±0.35	4.33
G13	0.60±0.22	3.99	0.43±0.23	2.69	0.16±0.24	1.44
PKC (Gq)	-0.09±0.20	0.80	0.55±0.20	3.52	-0.43±0.22	0.37
PKC (G11)	-0.10±0.19	0.79	0.61±0.19	4.09	-0.26±0.20	0.55
PKC (G14)	-0.63±0.56	0.24	-0.09±0.40	0.81	-0.59±0.52	0.26
PKC (G15)	-0.03±0.20	0.93	0.39±0.10	2.48	-0.47±0.22	0.34
β-arrestin 1	-0.11±0.17	0.78	0.25±0.17	1.76	-0.48±0.18	0.33
β-arrestin 2	-0.08±0.16	0.84	0.32±0.17	2.09	-0.31±0.18	0.49

Figure 1

Molecular Pharmacology Fast Forward. Published on July 2, 2022 as DOI: 10.1124/molpharm.122.000497
This article has not been copyedited and formatted. The final version may differ from this version.

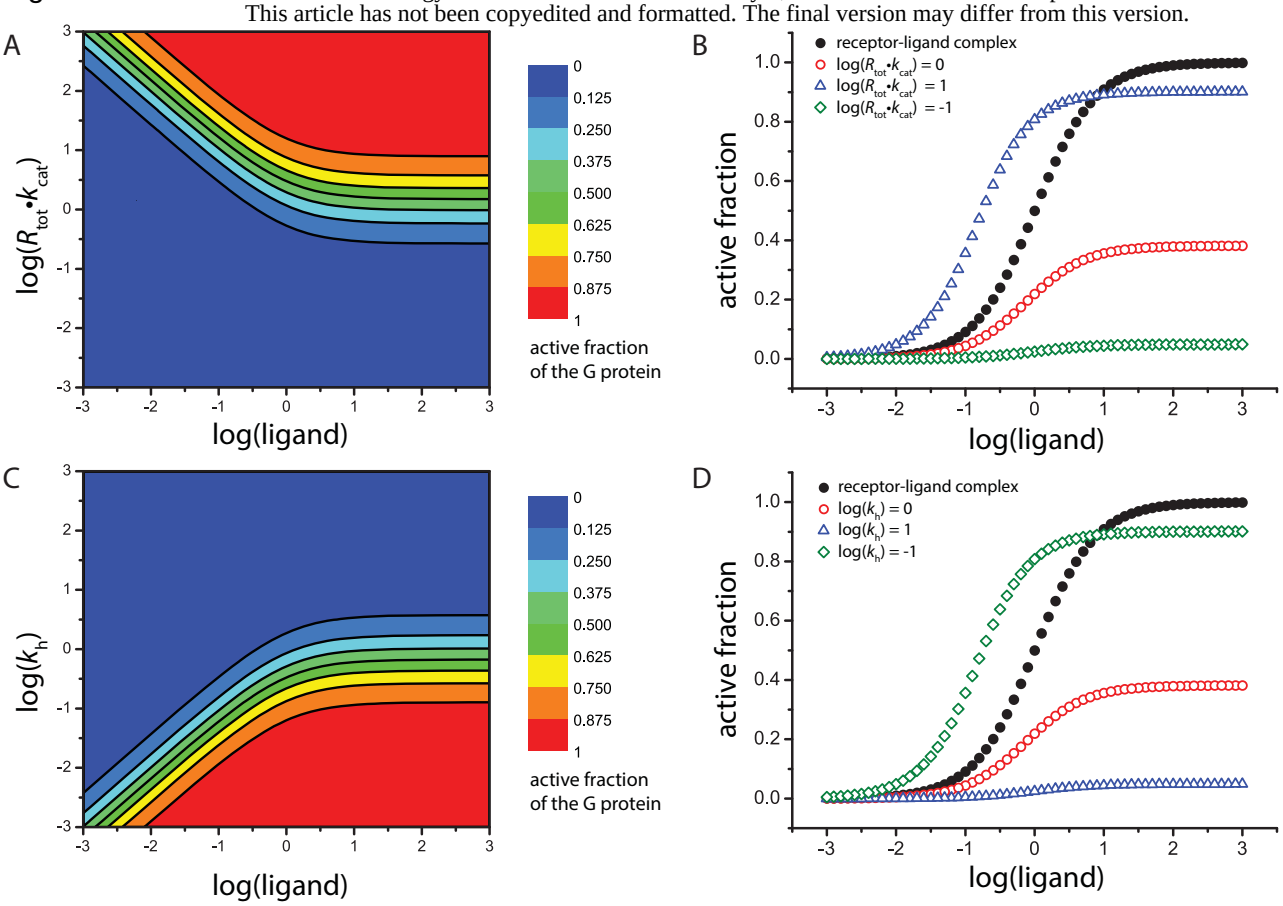

Figure 2

Molecular Pharmacology Fast Forward. Published on July 2, 2022 as DOI: 10.1124/molpharm.122.000497
This article has not been copyedited and formatted. The final version may differ from this version.

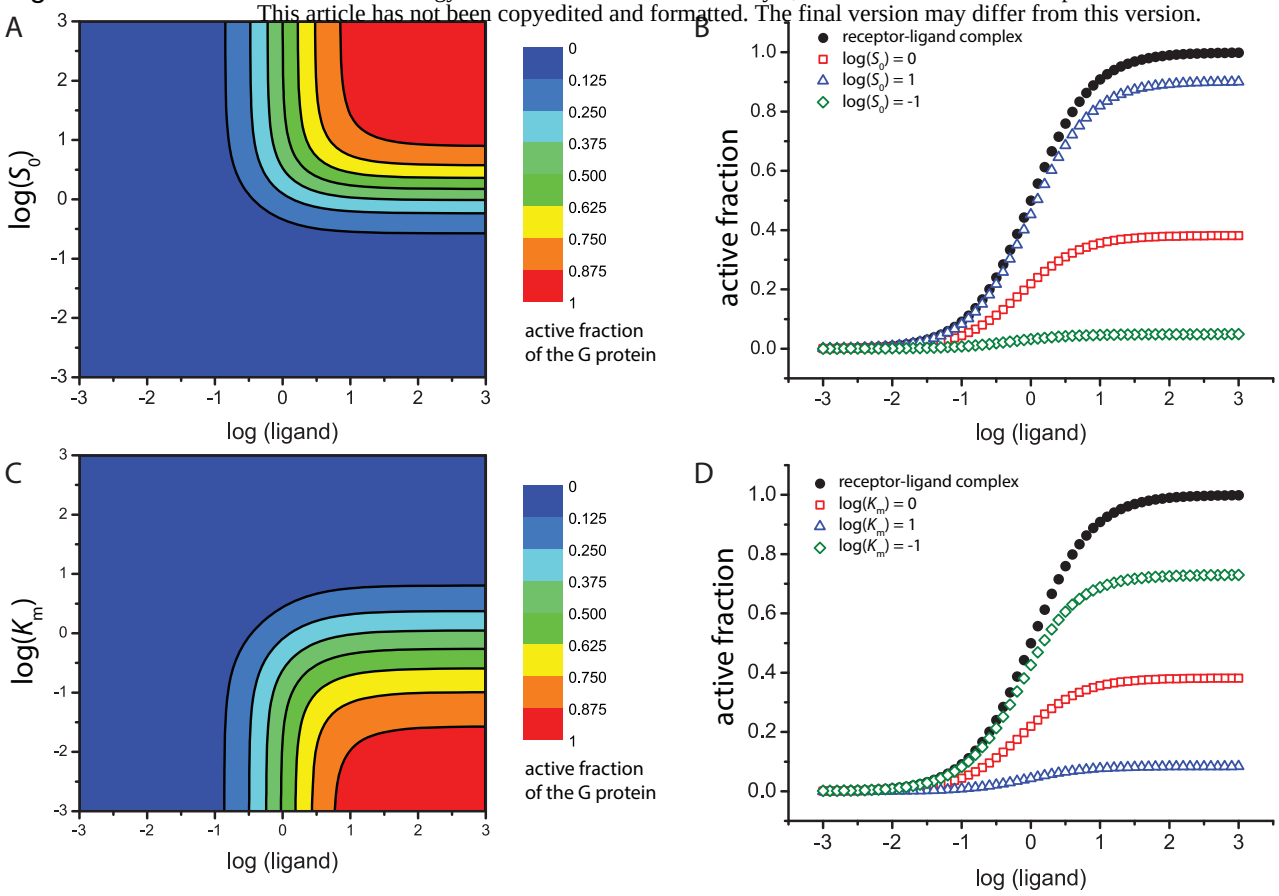

Figure 3

Molecular Pharmacology Fast Forward. Published on July 2, 2022 as DOI: 10.1124/molpharm.122.000497
This article has not been copyedited and formatted. The final version may differ from this version.

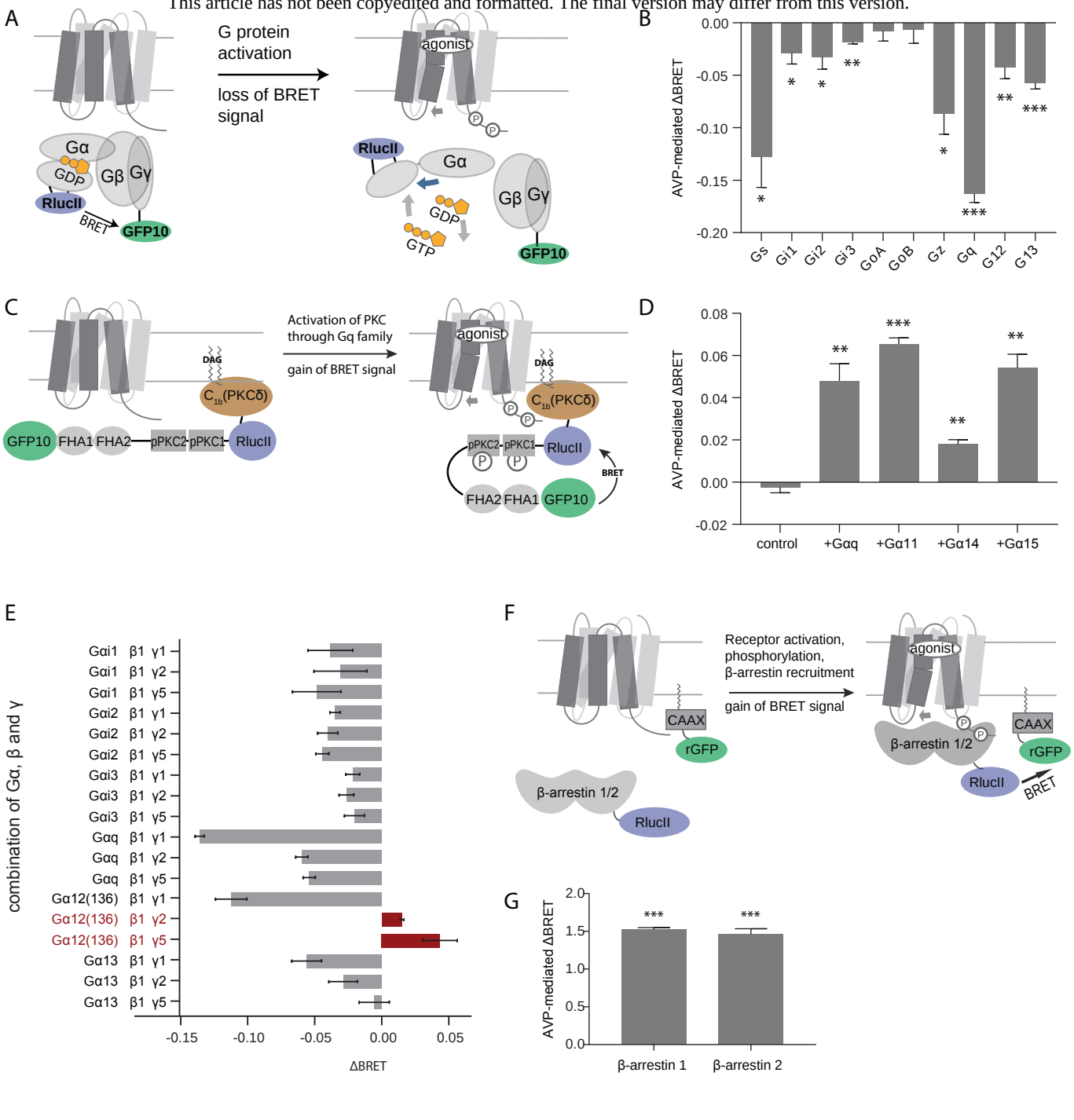

Figure 4